Reviews

Distortions in Octahedrally Coordinated d^0 Transition Metal Oxides: A Continuous Symmetry Measures Approach

Kang Min Ok and P. Shiv Halasyamani*

Department of Chemistry and the Center for Materials Chemistry, University of Houston, Houston, Texas 77204-5003

David Casanova, Miquel Llunell, Pere Alemany, and Santiago Alvarez*

Departament de Química Inorgànica Departament de Química Física, and Centre de Recerca en Química Teórica, Universitat de Barcelona, Martí i Franquès 1-11, 08028 Barcelona, Spain

Received February 27, 2006. Revised Manuscript Received April 24, 2006

More than 750 d^0 transition metal oxide octahedra have been examined in order to better understand the out-of-center distortion occurring with these cations. A continuous symmetry measures approach was used to quantify the magnitude and direction of the distortion. Using this approach we were able to divide the d^0 transition metals into three categories: strong (Mo^{6+} and V^{5+}), moderate (W^{6+}, Ti^{4+}, Nb^{5+}, and Ta^{5+}), and weak (Zr^{4+} and Hf^{4+}) distorters. We also examined and discussed the directional preference of the distortion for each cation.

Introduction and Background

In oxides, octahedrally coordinated d^0 transition metals, i.e., Ti^{4+}, Nb^{5+}, W^{6+}, etc., play a crucial role in a host of materials properties that is attributable to a distortion of the d^0 cation from the center of its oxide octahedron. This intra-octahedral distortion is the driving force for a variety of technologically important properties such as piezoelectricity, ferroelectricity, pyroelectricity, and nonlinear optical phenomena. The distortion can be attributed to second-order Jahn−Teller (SOJT) effects.[1−6] These effects occur when the empty d-orbitals of the metal mix with the filled p-orbitals of the oxide ligands. In extended structures, this mixing results from a spontaneous distortion of the metal cation that removes the near degeneracy of these two orbital sets. The metal cation displacement usually occurs along one of three directions, either toward an edge of the octahedron, a face, or a vertex.[7] Previously, we examined the magnitude and direction of this distortion in materials that contain both d^0 transition metals and a lone-pair cation, e.g., Se^{4+}, Te^{4+}, I^{5+}, etc.[8] We used a simple geometric formula to quantify the extent of the distortion. In addition, we determined that the magnitude of the distortion scales roughly with the electronegativity of the cation.[9]

In this article, we examine a variety of d^0 transition metal oxides, not limiting ourselves to materials that contain both a d^0 transition metal and a lone-pair cation. In this regard, we use more than 75 examples for each d^0 transition metal, except for Hf^{4+}, where only 27 examples could be found. More importantly, we employ continuous shape measures[10,11] to more-rigorously quantify the magnitude and direction of the distortion. As we will demonstrate, using this approach enables us to gain a much better description and understanding of the octahedral distortions.

Continuous Shape and Symmetry Measures. The continuous shape and symmetry measures (abbreviated CShM and CSM, respectively) proposed by Avnir[10−12] provide a way of quantitatively evaluating the degree of distortion of an atomic coordination sphere from some chosen ideal polyhedral shape or from a given symmetry. In short, the proposed method consists of finding the ideal structure with the desired shape (CShM) or symmetry (CSM) that is closest to the problem structure. Once at hand, the two polyhedra are superimposed in such a way as to minimize the expression in eq 1, which then gives the shape measure of the investigated structure Q relative to the ideal shape P, where $\vec{q}_i$ is an N vector that contains the 3*N* Cartesian coordinates of structure Q, $\vec{p}_i$ contains the coordinates of polyhedron P, and $\vec{q}_0$ is the position vector of the geometric center that is chosen to be the same for the two polyhedra.

$$S(\mathrm{Q,P}) = \min\left[\frac{\sum_{i=1}^{N}|\vec{q}_i - \vec{p}_i|^2}{\sum_{i=1}^{N}|\vec{q}_i - \vec{q}_0|^2}\right] \times 100 \qquad (1)$$

$S(\mathrm{Q,P}) = 0$ corresponds to a structure Q fully coincident in

* To whom correspondence should be addressed. E-mail: psh@uh.edu (P.S.H.) and Santiago.alvarez@qi.ub.es (S.A.).

10.1021/cm0604817 CCC: $33.50
Published on Web 06/02/2006

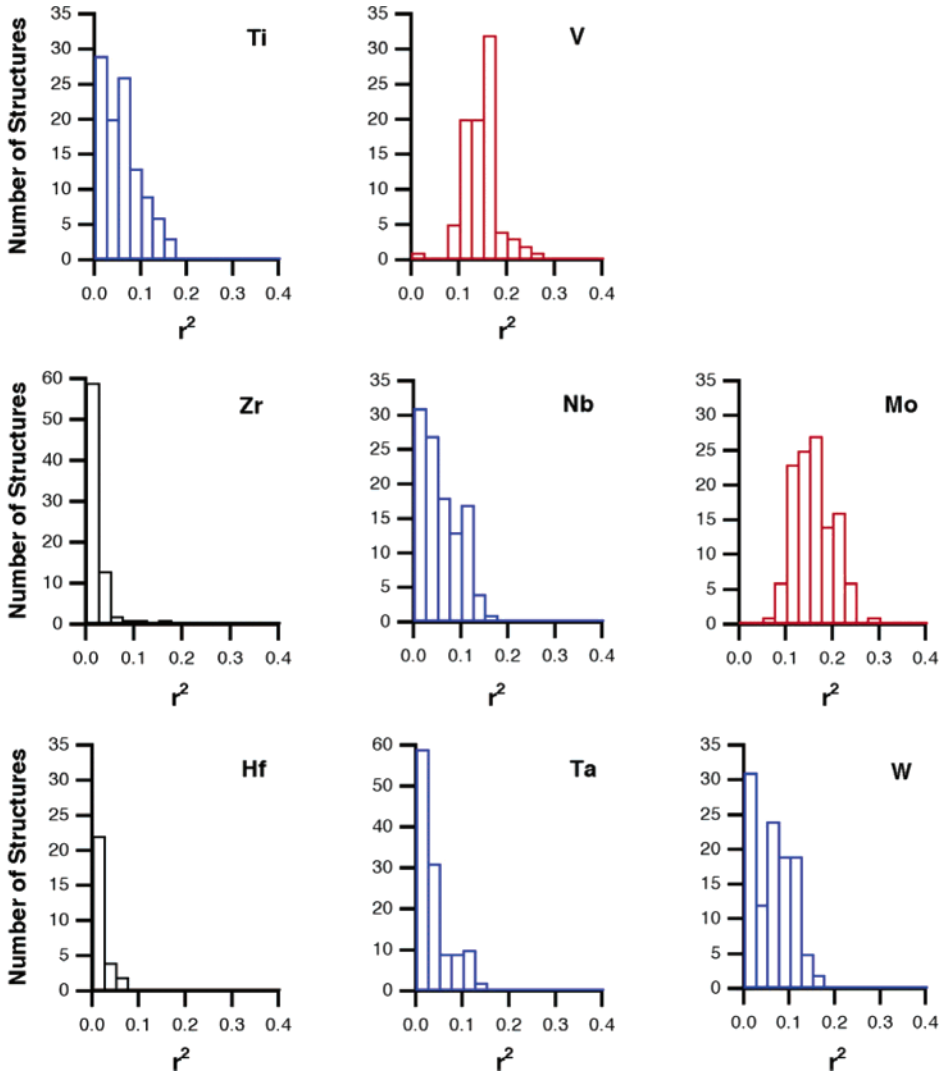

Figure 1. Distribution of the off-center displacements (r^2, in Å^2) for different d^0 metal ions in MO_6 octahedra. Color code: red, strong distorters; blue, moderate distorters; and black, weak distorters.

shape with the reference polyhedron P, regardless of size and orientation. The maximum allowed value is $S(Q,P) = 100$, although in practice the values found for severely distorted chemical structures are never larger than 50.

For the purpose of the present work, we can use several shape and symmetry measures to analyze the distortion of the MO_6 groups from the octahedron and the loss of inversion symmetry: the octahedral measures of the MO_6 group, $S(MO_6, O_h)$ and the O_6 group, $S(O_6, O_h)$; and the inversion symmetry measures of the O_6 group with and without the metal, $S(MO_6, i)$ and $S(O_6, i)$, respectively. In that way we can easily calibrate (a) the magnitude of the deviation from octahedricity of the MO_6 and O_6 groups, (b) whether such distortions imply a loss of inversion center, and (c) the magnitude of the deviation from centrosymmetry.

Because the calculation of the shape (symmetry) measures through eq 1 gives as a side product the displacement vectors of the real atoms from their positions in the ideal structure, we can analyze for each structure not only the presence and magnitude of the off-center distortion but also the direction of the metal atom displacement, be it toward a vertex, the center of an edge, the center of a face, or to intermediate directions. We have thus calculated the magnitude and direction of such a displacement vector that points from the center of the ideal O_6 octahedron to the position of the metal in the real structure, given as the square of its modulus (r^2) and as the angles between that vector and the vectors from the octahedral center to the vertex ($\vec{v}$), edge center ($\vec{e}$), and face center ($\vec{f}$), respectively (see the Supporting Information). For that task, we have to initially identify the atoms in each structure that correspond to the closest vertex (V_1), the closest edge (V_1 and V_2), and the closest face (V_1, V_2, and V_3) with regard to the central metal atom. Next, we define the vectors that go from the center of the octahedron to the closest vertex, to the center of the closest edge, and to the center of the closest face, as well as the vector that defines the displacement of the metal atom from the center of the octahedron to its actual position in the real structure. Finally, we calculate the angles between the displacement vector and the vertex, edge, and face vectors ($\vec{v}$, $\vec{e}$, and $\vec{f}$, respectively) for the ideal octahedron. Using the ideal octahedron to define the direction of the displacement vector is reasonable as long as the distortions of the O_6 octahedra are reasonably small, as is the case for all the structures studied here.

With all the data of the off-center distortion at hand (V_1, V_2, and V_3; $\vec{v}$, $\vec{e}$, and $\vec{f}$), we automatically assign the type of

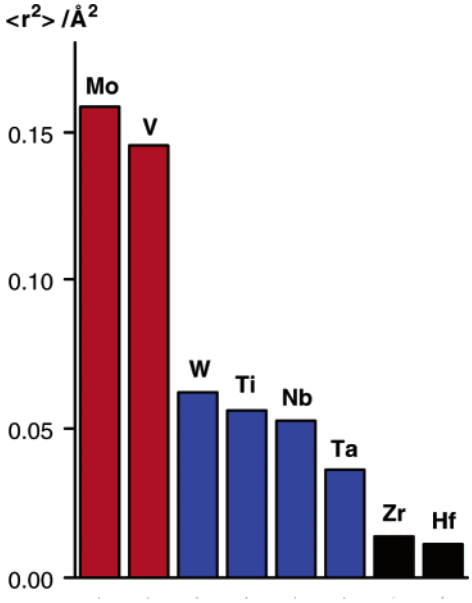

Figure 2. Average magnitude of the off-center distortions for individual d^0 transition metal cations.

distortion, as corresponding to vertex, edge, or face directions, or to intermediate directions, according to the following criteria: (a) MO_6 groups with off-center deviations of 0.01 Å or less are considered to be undistorted; (b) an off-center distortion is assigned to the direction that gives the smallest angle, provided the other two angles exceed it by at least a factor of 1.2; and (c) distortions that present at least two similar angles are considered to be intermediate. All these calculations were performed with a modified version of the SHAPE program[13] made specifically for the analysis of off-center distortions of the octahedron, providing as input data the Cartesian coordinates of each unique MO_6 octahedron. We examined a total of 762 MO_6 crystallographically independent octahedra corresponding to d^0 transition metal ions in 394 crystal structures.

Octahedral Distortions. The first two questions we wish to address concern the magnitude and direction of the d^0 transition metal distortion. Histograms showing the distribution of the off-center displacements (represented as the squared modulus of the displacement vector, for reasons to be discussed below) found for each studied metal ion are presented in Figure 1. From Figure 1, we observe that the d^0 metal ions can be classified into three different groups according to the distribution of their off-center distortions: (i) V^{5+} and Mo^{6+}, which show maxima at values of r^2 close to 0.2 Å^2, with practically no undistorted structures; (ii) Ti^{4+}, Nb^{5+}, Ta^{5+}, and W^{6+}, with distribution maxima close to the undistorted structure, but off-center distortions extending up to r^2 values of around 0.2 Å^2; and (iii) Zr^{4+} and Hf^{4+}, with mostly undistorted structures and practically all r^2 values less than 0.1 Å^2. The information displayed in Figure 1 can be summarized by plotting the mean r^2 value for each of the eight d^0 transition metals studied, as shown in Figure 2. As seen, the average distortion for the d^0 cations scale as follows

$$Mo^{6+} \approx V^{5+} \gg W^{6+} \approx Ti^{4+} \approx Nb^{5+} > Ta^{5+} \gg Zr^{4+} \approx Hf^{4+}$$

The trend is consistent with what we observed earlier.[8] In addition, this trend scales with the electronegativity of the cation, as determined by Woodward et al.[9] In other words, the more electronegative the cation, the greater, on average, the distortion. Thus, the cations may be divided into three groups, strong distorters (Mo^{6+} and V^{5+}, comprising 206 data sets), moderate distorters (W^{6+}, Ti^{4+}, Nb^{5+}, and Ta^{5+}, comprising 452 data sets), and weak distorters (Zr^{4+} and Hf^{4+}, comprising 104 data sets).

Table 1. Number of Directional Distortions with Respect to Individual Cation

cation	vertex	edge	face	undistorted	intermediate	total
Mo^{6+}	0	91	22	0	6	119
V^{5+}	51	33	0	0	3	87
W^{6+}	13	45	29	10	16	113
Ti^{4+}	37	35	13	13	10	108
Nb^{5+}	37	25	23	12	14	111
Ta^{5+}	28	44	14	24	10	120
Zr^{4+}	8	13	20	31	5	77
Hf^{4+}	0	6	6	13	2	27
total	174	292	127	103	66	762

Table 2. Percentage of Directional Distortions with Respect to Individual Cation

cation	vertex	edge	face	undistorted	intermediate
Mo^{6+}	0	76	19	0	5
V^{5+}	59	38	0	0	3
W^{6+}	11	40	26	9	14
Ti^{4+}	34	32	12	12	9
Nb^{5+}	33	22	21	11	13
Ta^{5+}	23	37	12	20	8
Zr^{4+}	10	17	26	40	6
Hf^{4+}	0	22	22	48	7

With respect to the direction of the distortion, vertex, edge, or face, we also observe interesting trends. Table 1 presents the raw data classified according to cation and direction of the metal distortion: vertex, edge or face. The fifth column reflects the number of instances in which the cations remain undistorted, i.e., at the center of its oxide octahedron. Finally, in a number of cases, even if there is a non-negligible off-center distortion, the cation cannot be unambiguously ascribed to one of the special directions of the octahedron and is classified as intermediate. The cations in Table 1 are ordered by strength of distortion, from strong to weak, according to the average values of Figure 2. To examine Table 1, we rather look at the percentages of the distortions within each cation. In other words, how often does a specific cation distort toward a vertex, edge, or face? This information is given in Table 2. A few points are of note. As we move from strong to weak distorters, i.e., Mo^{6+} to Hf^{4+}, the probability for an undistorted geometry greatly increases. *All* 206 examples with Mo^{6+} and V^{5+} have the cation distorted from the center of its oxide octahedron, whereas for Zr^{4+} and Hf^{4+}, a sizeable fraction, 40 and 48%, respectively, of the examples exhibit an undistorted environment. This is perhaps not too surprising, given the weakness of the average metal cation distortion for the latter two cations. If we examine the distortion for individual cations, we note that for Mo^{6+}, W^{6+}, Zr^{4+}, and Hf^{4+}, edge and face distortions are strongly preferred over corner displacements. With the Nb^{5+}, Ti^{4+}, and Ta^{5+} cations, the directionality of the distortions are divided roughly equally between the three directions. In contrast, no examples are found of face-distorted V^{5+} cations. Surprisingly, for the strong distorters,

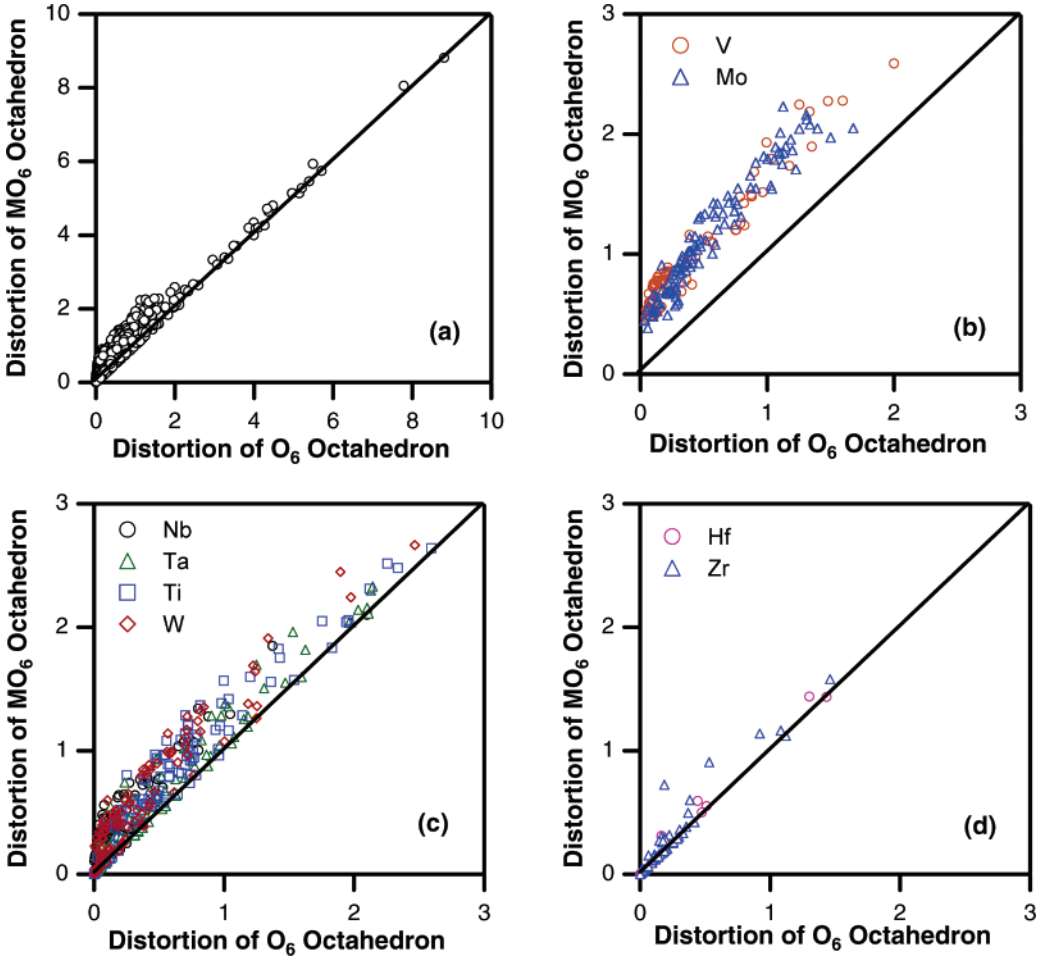

Figure 3. Scatterplot of the distortions of the MO_6 and O_6 octahedra, $S(MO_6, O_h)$ and $S(O_6, O_h)$, for (a) all eight d^0 transition metal cations, and those classified as (b) strong distorters (Mo^{6+} and V^{5+}), (c) moderate distorters (W^{6+}, Nb^{5+}, Ta^{5+}, and Ti^{4+}), and (d) weak distorters (Zr^{4+} and Hf^{4+}).

there are only a few structures that can be classified as intermediate distortions, with most cases being distinctly classified as vertex, edge, or face distortions. It is worth stressing that, even if we classify both Mo^{6+} and V^{5+} as strong distorters, the preferred directions of the off-center distortions are quite different for these two metal ions (Table 2).

We have so far worried about the displacement of the metal ion from the center of the O_6 ligand set, regardless of whether it is a perfect octahedron or not. It is appropriate to ask now if the off-center displacement of the metal cation is in some way associated with a distortion of the coordination polyhedron. A scatterplot of the octahedral distortions of the MO_6 and O_6 groups in each structure is shown in Figure 3a. The position of a given structure in that scatterplot provides us with information about the type of distortion, as schematically summarized in Scheme 1. (a) The diagonal line corresponding to $S(MO_6, O_h) = S(O_6, O_h)$ represents geometries in which the MO_6 and O_6 octahedra experience the same amount of distortion, indicating that the metal atom remains at the octahedral center; (b) the vertical axis represents those structures in which the O_6 ligand set remains perfectly octahedral while the MO_6 group is increasingly distorted, thus corresponding to pure displacements of the metal atom from the center of the undistorted ligands' octahedron; (c) in the regions between these two lines, both distortions are present. Let us mention that all structures must obey the

Scheme 1

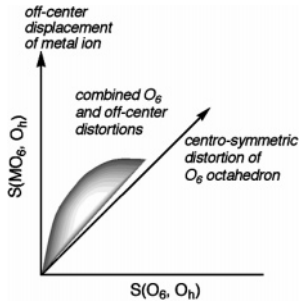

relationship $S(MO_6, O_h) \geq S(O_6, O_h)$, because adding a metal atom at the center of the octahedron amounts to adding the same term to the numerator and the denominator of eq 1. Indeed, for all 762 of the MO_6 octahedra examined, the metal cation distortion is equal to or greater than the oxide ligand distortion. To further analyze the data of Figure 3a, we can separate the data into three groups that correspond to strong (Mo^{6+} and V^{5+}), moderate (W^{6+}, Ti^{4+}, Nb^{5+}, and Ta^{5+}), and weak (Zr^{4+} and Hf^{4+}) distorters, presented in Figures 3b−d, respectively; we focused only on the region of small values of the symmetry measures to best appreciate the differences.

Let us look first at the data in the group of strong distorters (Mo^{6+} and V^{5+}, Figure 3b). We notice that the points lie well above the bisecting line, in the zone corresponding to geometries that present both a distortion of the O_6 octahedron and a displacement of the metal atom from the octahedral

center. However, all the octahedral shape measures for these two cations appear within the window shown, with values less than 3, indicating that only moderate distortions of the O_6 group are present. For cations in the group of moderate distorters (W^{6+}, Ti^{4+}, Nb^{5+}, and Ta^{5+}, Figure 3c), even if one can find more-pronounced distortions of the octahedra (with $S(O_6, O_h)$ values of up to 6, outside the plot range), the fact that the points appear closer to the diagonal indicate smaller displacements of the metal atom from the octahedron center, as corresponds to the r^2 values found (Figures 1 and 2). For the last group, that of the weak distorters (Zr^{4+} and Hf^{4+}, Figure 3d), we notice that the majority of data lie on the bisecting line (corresponding to $r^2 \approx 0$), even if distortions of the O_6 octahedra corresponding to $S(O_6, O_h)$ values as high as 10 can be found. We must be cautious about our conclusions regarding the family of weak distorters, because the number of analyzed data points is smaller in this case than for the other two families. In all three cases, strong, moderate, and weak distorters, we have kept the same scale for both axes to facilitate comparisons.

The above analysis of the octahedral measures indicates that two types of distortions are present in the structures studied, that of the O_6 octahedron and the off-center displacement of the metal ion. This conclusion is further supported by comparison of the $S(O_6, O_h)$ and r^2 values, which shows that these two parameters are *uncorrelated*. Let us now then focus on the distortions of the O_6 groups, disregarding the metal atom. This can be done by looking at the octahedral measures, $S(O_6, O_h)$, for each of the transition elements considered, as summarized in the histograms of Figure 4. There it can be seen that the strong distorter metal ions (Mo^{6+} and V^{5+}) are not among the strongest distorters of the O_6 octahedron. The whole series can be ordered according to the tendency to distort the O_6 octahedron, taking into account the average $S(O_6, O_h)$ values for the different cations and their standard deviations

$$[Hf^{4+}] \approx Ta^{5+} > Ti^{4+} > Mo^{6+} \approx V^{5+} \approx W^{6+} \approx Zr^{4+} > Nb^{5+}$$

where Hf^{4+} appears in brackets to indicate that the smaller number of available data introduces some uncertainty about its position in this series. Clearly this trend bears little resemblance to the magnitude of the out-of-center distortions for each d^0 cation.

We have so far gained a great deal of information about the distortion of the metal coordination spheres by analyzing the loss of octahedricity of the MO_6 and O_6 groups and the degree of off-center displacement of the metal atom. Let us recall, however, that some relevant physical properties of these oxide materials are related to the absence of an inversion center, such as second-harmonic generation, piezoelectricity, and ferroelectricity. We should now then try to go one step further and investigate how acentric (i.e., how far from having an inversion center) those metal coordination spheres are. We must not forget, though, that the existence of acentric building blocks as the distorted MO_6 groups is a necessary but not sufficient condition for having an acentric crystal structure.

It is interesting to plot $S(MO_6, O_h)$ vs $S(O_6, O_h)$, as in Figure 3, for eight well-known noncentrosymmetric oxides: $NaNbO_3$,[14] $KNbO_3$,[15] $BaTiO_3$,[16] $LiTaO_3$,[17] $KTiOPO_4$,[18] $PbZrO_3$,[19] $PbTiO_3$,[20] and $LiNbO_3$.[21] We observe that all of the points, with the exception of $NaNbO_3$, lie substantially above the bisecting line (see Scheme 2) and present relatively weak distortions of the O_6 octahedron, suggesting that what is important for the acentric properties is to have a significant off-center displacement of the metal ion but that the loss of octahedricity of the oxide ions has a minor effect. If we examine these points more closely, we note that the larger the *y*-axis value, the larger the ferroelectric spontaneous polarization. It should be noted that $KTiOPO_4$ is not ferroelectric at room temperature because of ionic conductivity,[22] whereas $PbZrO_3$ and $NaNbO_3$ are antiferroelectric. The correlation of the spontaneous polarization with the distortion of the d^0 metal cation is consistent with earlier reports.[23]

Because acentric properties of d^0 metal oxides are related to the presence or absence of an inversion center, one can expect that the degree of deviation from inversion symmetry might be in some way related to the magnitude of the polarizing power. We have therefore calculated the inversion measures of the MO_6 and O_6 octahedra. No correlation was found between those inversion measures and the corresponding octahedral measures or their off-center displacements. This is not an unexpected result, given the presence of two types of distortions in the metal-coordination spheres, either independently or combined. To remove part of the acentricity attributable to the arrangement of the oxide ions, we take the difference of the inversion measures of the MO_6 and O_6 groups in each structure and plot it as a function of the square of the off-center displacement (Figure 5). An excellent linear correlation is found between the displacement of the metal ion and the increase in acentric character upon incorporation of the metal atom to the O_6 octahedron. It can be shown that the linear correlation in Figure 5 is a consequence of the definition of the two inversion measures, provided the differences in size of the polyhedra considered are small (see the Appendix). From the least-squares fitting equation of Figure 5, we can establish to a good approximation that the loss of inversion symmetry of the MO_6 group can be expressed as the sum of the loss of inversion symmetry of the O_6 octahedron and the off-center displacement of the metal ion (eq 2). Inspection of those two contributions for the structures analyzed shows that there are nearly equal proportions of compounds in which the acentricity is dominated by the ligands' distortion ($S(O_6, i)$ term in eq 2) and compounds in which the dominant term is the metal displacement, with the two factors having approximately the same weight in some 12% of cases.

$$S(MO_6, i) \approx S(O_6, i) + 3.782r^2 \quad (2)$$

A similar correlation to that shown in Figure 5 can be found between the square of the off-center displacement and the difference in octahedral measures of the MO_6 and O_6 groups. An interesting outcome of the definition of continuous symmetry measures (eq 1) is that the loss of inversion symmetry associated with the off-center displacement of the metal ion depends only on the magnitude of such displacement (r^2) and not on its direction (vertex, edge, or face). Consider the case of the strong distorters, Mo^{6+} and V^{5+};

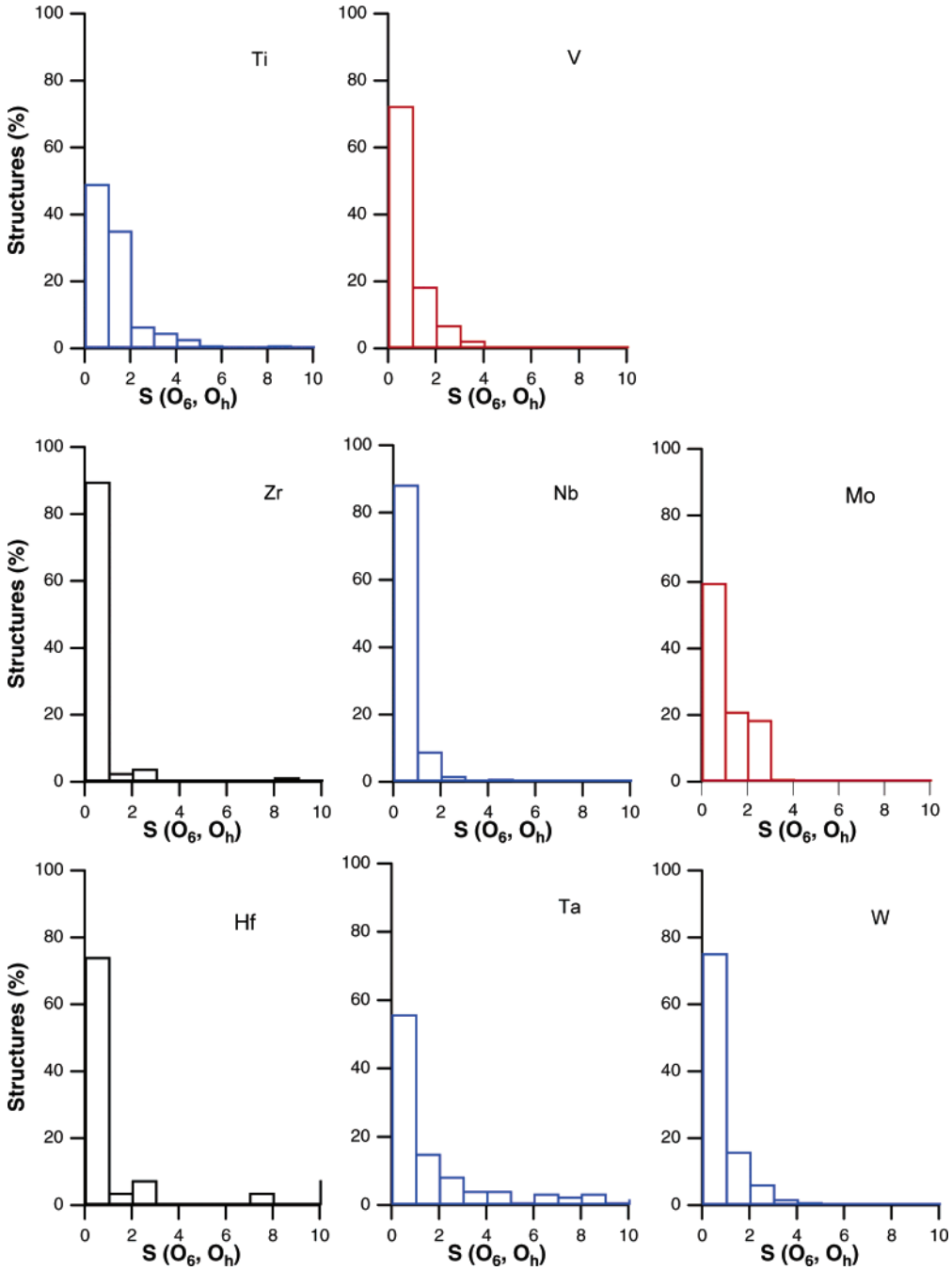

Figure 4. Distribution of the distortions from the octahedron of the O_6 groups in different d^0 metal oxides. Color code is as in Figure 1.

even if the former is not found with the metal displaced in the vertex direction and the latter is never found distorted toward a face, both present a similar distribution of r^2 and $S(MO_6$, inversion) values.

Conclusions

The continuous symmetry measures approach allows us to calculate in an accurate and unequivocal way the displacement of the metal atom from the center of the ideal O_6 octahedron in d^0 metal oxides, regardless of the type and degree of deviation of the ligand set from octahedral symmetry. Alternative measures of the off-center distortion are the differences in octahedral or inversion symmetry measures between the MO_6 and O_6 groups, i.e., $S(MO_6, R) - S(O_6, R)$, where $R = O_h$ or inversion, that present linear correlations with r^2.

On the basis of the presented data, we can draw several conclusions. First, with the d^0 transition metal oxide octahedra, two types of distortions are observed. These distortions are off-center displacements of the metal cation and a distortion of the O_6 polyhedron with respect to the regular octahedron. It is important to note that these distortions are *uncorrelated*. With the former, the d^0 metal cations can be divided into strong (Mo^{6+} and V^{5+}), moderate (W^{6+}, Ti^{4+}, Nb^{5+}, and Ta^{5+}), and weak (Zr^{4+} and Hf^{4+}) distorters. In addition, the directional preference of the distortion, toward a vertex, edge, or face, for each cation has been determined. For V^{5+}, distortions toward an edge or vertex are common, with face-directed distortions, interestingly, never observed, whereas for Mo^{6+} and Hf^{4+} only edge- or face-directed distortions are observed. With the other cations, W^{6+}, Ti^{4+},

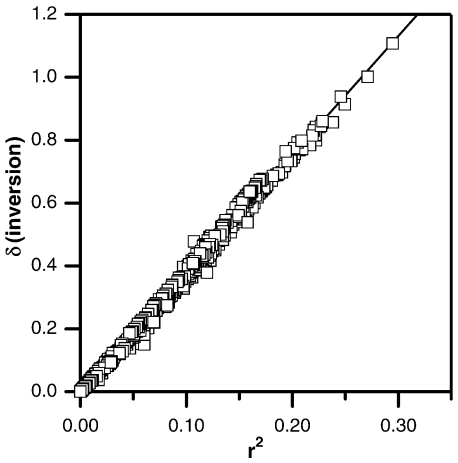

Figure 5. Difference of the inversion measure of the MO_6 and O_6 octahedra as a function of the square of the off-center displacement of the metal atom (in Å^2). δ(inversion) is defined as $S(MO_6, i) - S(O_6, i)$. Least-squares fitting gives $\delta(\text{inversion}) = 3.782(8)r^2 - 0.003(1)$.

Scheme 2

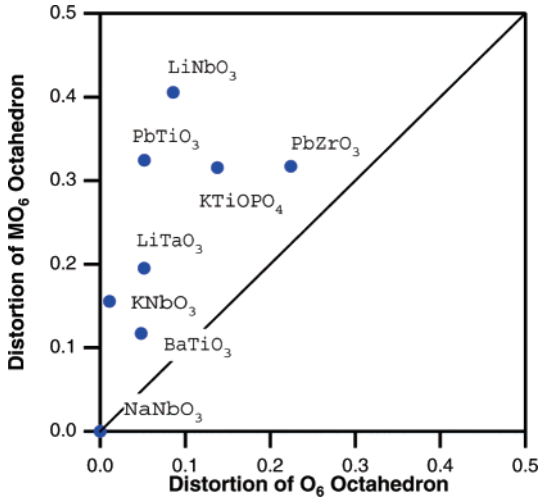

Table 3. Summary of the Distortions of the MO_6 Octahedra Classified by Metal Ions

cation	direction	off-center distortion[a]	O_6 distortion
Mo^{6+}	edge (preferred), face	strong (0.158)	less frequent
V^{5+}	vertex, edge	strong (0.145)	less frequent
W^{6+}	edge preferred	moderate (0.062)	less frequent
Ti^{4+}	any	moderate (0.056)	frequent
Nb^{5+}	any	moderate (0.053)	less frequent
Ta^{5+}	any	moderate (0.036)	frequent
Zr^{4+}	any	weak (0.014)	less frequent
Hf^{4+}	edge, face	weak (0.011)	frequent

[a] The average value of the average off-center distortion ($\langle r^2 \rangle$ in Å^2) for each metal ion is given in parentheses

Nb^{5+}, and Ta^{5+}, the three directions, vertex, edge, and face, can be found in similar proportions. All of this information is summarized in Table 3. With respect to the oxide (O_6) octahedron distortion, the distortion scales as $[Hf^{4+}] \approx Ta^{5+} > Ti^{4+} > Mo^{6+} \approx V^{5+} \approx W^{6+} \approx Zr^{4+} > Nb^{5+}$ (see Figure 4). This indicates, as stated earlier, that the two types of distortions are completely uncorrelated.

Acknowledgment. D.C., M.L., P.A., and S.A. thank the Dirección General de Enseñanza Superior (DGES-MEC, Grant CTQ2005-08123-C02/BQU) and Comissió Interdepartamental de Ciència i Tecnologia (CIRIT, Grant 2005SGR-00036). K.M.O. and P.S.H. thank the Robert A. Welch Foundation, the NSF Career Program (DMR-0092054), and the NSF Chemical Bonding Center for support. Discussion and encouragement from D. Avnir (Institute of Chemistry, The Hebrew University of Jerusalem) in the initial phases of this work are highly appreciated by the authors.

Appendix: Relationship between Inversion Measures and the Off-Center Distortion

The inversion measures of the MO_6 and O_6 atomic sets, $S(MO_6, i)$ and $S(O_6, i)$, provide a quantitative scale for gauging their deviations from the closest related structure that has inversion symmetry. Then, in some way, the difference between these two measures should provide a calibration of the contribution of the central atom to the acentricity of the MO_6 group. From the mathematical expressions of $S(O_6, i)$ and $S(MO_6, i)$ in eq 1, we can deduce an approximate relationship between the square of the metal displacement vector (r^2) and the difference in inversion measures of the MO_6 and O_6 groups, δ(inversion), given in eq A.1.

$$\delta(\text{inversion}) = S(MO_6,i) - S(O_6,i) \approx \frac{6a}{7^2} r^2 \qquad \text{(A.1)}$$

$$a = \frac{7}{\sum_{i=1}^{7} |\vec{q}_i - \vec{q}_0|^2} \qquad \text{(A.2)}$$

In eq. A.1, a is a term related to the size of the O_6 group (eq A.2, where $\vec{q}_i$ are the vectors that contain the atomic coordinates of the MO_6 group, and $\vec{q}_0$ is the vector of its geometric center). Deviations from the linear dependence on r^2 found in Figure 5 are therefore associated with the different atomic radii of the studied metals; those differences are small enough to make a approximately constant for the whole series of structures investigated, which results in the excellent linear correlation shown in Figure 5. Notice that if the inversion measures of the MO_6 and O_6 groups are identical (i.e., $\delta(\text{inversion}) = 0$), then the metal atom must be at the center of the ligand set ($r^2 = 0$), which explains the absence of an independent term in eq A.1 and is in excellent agreement with the very small value found in the least-squares fitting expression of Figure 5. We notice also that a has units of the inverse of the square of a distance, and thus δ(inversion) is adimensional. The same reasoning can be applied to the octahedral measures, which accounts for the similar linear correlation found between $\delta(O_h)$ and r^2.

Supporting Information Available: Spreadsheets with the magnitude and direction of the cation distortions have been deposited. This material is available free of charge via the Internet at http://pubs.acs.org.

References

(1) Opik, U.; Pryce, M. H. L. *Proc. R. Soc. London, Ser. A* **1957**, *238*, 425−447.
(2) Bader, R. F. W. *Mol. Phys.* **1960**, *3*, 137−151.
(3) Bader, R. F. W. *Can. J. Chem.* **1962**, *40*, 1164−1175.
(4) Pearson, R. G. *J. Am. Chem. Soc.* **1969**, *91*, 4947−4955.
(5) Pearson, R. G. *J. Mol. Struct. (THEOCHEM)* **1983**, *103*, 25−34.
(6) Wheeler, R. A.; Whangbo, M.-H.; Hughbanks, T.; Hoffmann, R.; Burdett, J. K.; Albright, T. A. *J. Am. Chem. Soc.* **1986**, *108*, 2222−2236.

(7) Goodenough, J. B. *Annu. Rev. Mater. Sci.* **1998**, *28*, 1−27.
(8) Halasyamani, P. S. *Chem. Mater.* **2004**, *16*, 3586−3592.
(9) Eng, H. W.; Barnes, P. W.; Auer, B. M.; Woodward, P. M. *J. Solid State Chem.* **2003**, *175*, 94−109.
(10) Zabrodsky, H.; Peleg, S.; Avnir, D. *J. Am. Chem. Soc.* **1992**, *114*, 7843.
(11) Alvarez, S.; Alemany, P.; Casanova, D.; Cirera, J.; Llunell, M.; Avnir, D. *Coord. Chem. Rev.* **2005**, *249*, 1693.
(12) Alvarez, S.; Avnir, D.; Llunell, M.; Pinsky, M. *New J. Chem.* **2002**, *26*, 996−1009.
(13) Llunell, M.; Casanova, D.; Cirera, J.; Bofill, J. M.; Alemany, P.; Alvarez, S.; Pinsky, M.; Avnir, D. *Shape Program*, version 1.1; University of Barcelona: Barcelona, Spain, 2003.
(14) Seidel, P.; Hoffman, W. *Z. Kristallogr.* **1976**, *143*, 444.
(15) Hewat, A. W. *J. Phys. C* **1973**, *6*, 1074−1078.
(16) Shirane, G.; Danner, H.; Pepinsky, R. *Phys. Rev.* **1957**, *105*, 846−855.
(17) Abrahams, S. C.; Bernstein, J. C. *J. Phys. Chem. Solids* **1967**, *28*, 1965−1977.
(18) Tordjman, I.; Masse, R.; Guitel, J. C. *Z. Kristallogr.* **1974**, *139*, 103−115.
(19) Fujishita, H.; Katano, S. *Ferroelectrics* **1998**, *217*, 17−20.
(20) Shirane, G.; Pepinsky, R.; Frazer, B. C. *Acta Crystallogr.* **1956**, *9*, 131−140.
(21) Maker, P. D.; Terhune, R. W.; Nisenoff, M.; Savage, C. M. *Phys. Rev. B.* **1962**, *8*, 21−35.
(22) Jiang, Q.; Womersley, M. N.; Thomas, P. A.; Rourke, J. P.; Hutton, K. B.; Ward, R. C. C. *Phys. Rev. B* **2002**, *66*, 094102/094101−094102/094108.
(23) Abrahams, S. C.; Kurtz, S. K.; Jamieson, P. B. *Phys. Rev.* **1968**, *172*, 551−553.

CM0604817